ACS Macro Letters

Letter

pubs.acs.org/macroletters

Well-Defined Ambipolar Block Copolymers Containing Monophosphorescent Dye

Nam-Goo Kang, Beom-Goo Kang, Yong-Guen Yu, Mohammad Changez, and Jae-Suk Lee*

Department of Nanobio Materials and Electronics, School of Materials Science and Engineering, Gwangju Institute of Science and Technology (GIST), 1 Oryong-Dong, Buk-Gu, Gwangju 500-712, Korea

Supporting Information

ABSTRACT: Well-defined ambipolar block copolymers containing carbazole, oxadiazole moieties, and only one homoleptic iridium(III) complex between the carbazole and oxadiazole blocks were successfully synthesized by sequential living anionic polymerization with controlled molecular weights (*M*w), a narrow molecular weight distribution (M_w/M_n < 1.15), and a high conversion yield (98−100%). The optimum conditions for the successful controlled synthesis of an oxadiazole-containing the homopolymer of poly(2-phenyl-5-(6-vinylpyridin-3-yl)-1,3,4-oxadiazole) have been established by controlling the nucleophilicity strength of the carbanion. In addition, the location and concentration of the homoleptic iridium(III) complex were controlled by linking it to 1,1-diphenylethylene, which exhibits monoaddition characteristics in the main chain of the block copolymer.

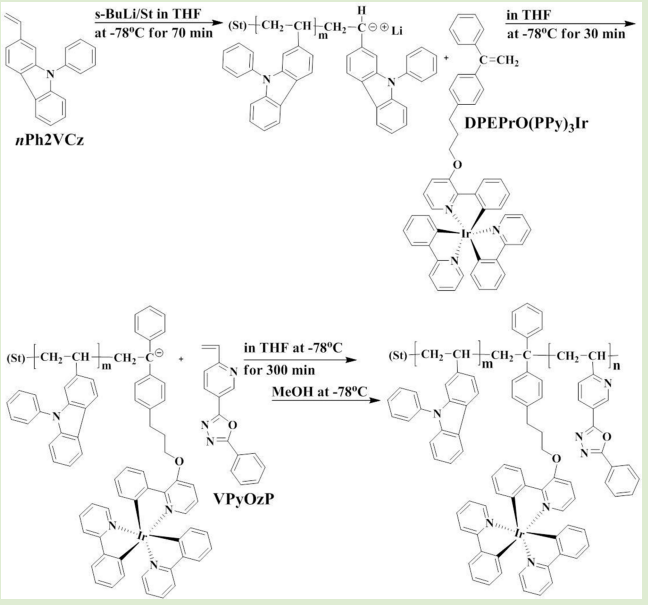

Living anionic polymerization is one of the most effective methods for preparing well-defined polymers with predictable molecular weights and narrow molecular weight distributions.[1] Using this technique, functional polymers containing nitrogen, oxygen, sulfur, and so on have been successfully synthesized.[2] However, attention must be paid to suppressing complicated side reactions caused by initiators, living polymer ends, and heteroatom-containing units. For example, although the anionic polymerization of 9-vinylcarbazole (NVK) is known to be impossible, the successful syntheses of uncontrolled poly(9-vinylcarbazole)[3] and a few controlled carbazole derivative polymers[4,5] by anionic polymerization have been reported.

In general, 1,3,4-oxadiazole-containing materials have been extensively utilized as acceptors because of their high electron-accepting characteristics as compared with oxazoles and triazoles.[6] Therefore, the synthesis by random or living radical polymerization of various polymethacrylates and polystyrenes bearing oxadiazoles as side chains has been reported.[7] However, the synthesis of controlled oxadiazole-containing polymers by anionic polymerization has not yet been reported due to complicated side reactions caused by the highly reactive carbanion of living polystyrene, *sec*-butyl lithium and so on.

1,1-Diphenylethylene (DPE) is one of styrene derivatives. However, anionic polymerization does not occur in an excess of DPE because DPE exhibits only monoaddition behavior. Combining functionalized DPE derivatives with living polymers could provide several methods for the preparation of chain-end-functionalized and in-chain-functionalized polymers with controlled structures.[8] Therefore, various DPE derivatives containing functional groups such as alcohols, amines, carboxylic acids, *N*,*N*-diisopropylamide, and so on have been introduced,[2a] but the synthesis and introduction of transition-metal-containing DPE in anionic polymerizations has not been studied.

Ambipolar block copolymers have been exploited as materials that can substantially improve the performance of organic electronics.[9] Although ambipolar block copolymers prepared by living radical polymerization demonstrated improved performance with respect to charge transport, as compared with random copolymers,[10] some synthetic limitations were discovered. In the synthesis of iridium complex (Ir)-containing ambipolar block copolymers, limitations were

Received: March 15, 2012
Accepted: June 12, 2012
Published: June 19, 2012

identified relating to (i) a decrease of the initiating block, (ii) a failure to initiate the second block, and (iii) a competition between termination and polymerization by nitroxide end groups or the postpolymerization attachment of the prepared Ir complexes.[11] Therefore, the synthesis of controlled ambipolar block copolymers by living polymerization remains a challenge. Control over the morphology is considered a key factor[12] because the morphologies of ambipolar block copolymers have a significant effect on their photophysical and electrical performance.[13]

In this study, we reported the synthesis of well-defined ambipolar block copolymers with 9-phenyl-2-vinyl-9*H*-carbazole (*n*Ph2VCz), (2-phenyl-3-(3-(4-(1-phenylvinyl)phenyl)-propoxy)pyr-idine)(2-phenylpyridine)$_2$iridium (DPEPrO-(PPy)$_3$Ir) with monoaddition characteristics, and 2-phenyl-5-(6-vinylpyridin-3-yl)-1,3,4-oxadiazole (VPyOzP) by a sequential living anionic polymerization, as shown in Scheme 1. We have demonstrated for the first time that the living anionic polymerization of Ir-containing and oxadiazole-containing monomers could be performed without any observable side reactions.

Scheme 1. Synthesis of Well-Defined Block Copolymers Containing 9-Phenyl-2-vinyl-9*H*-carbazole (*n*Ph2VCz), (2-Phenyl-3-(3-(4-(1-phenylvinyl)phenyl)propoxy)pyridine)(2-phenylpyridine)$_2$iridium (DPEPrO(PPy)$_3$Ir), and 2-Phenyl-5-(6-vinylpyridin-3-yl)-1,3,4-oxadiazole (VPyOzP) by Sequential Living Anionic Polymerization

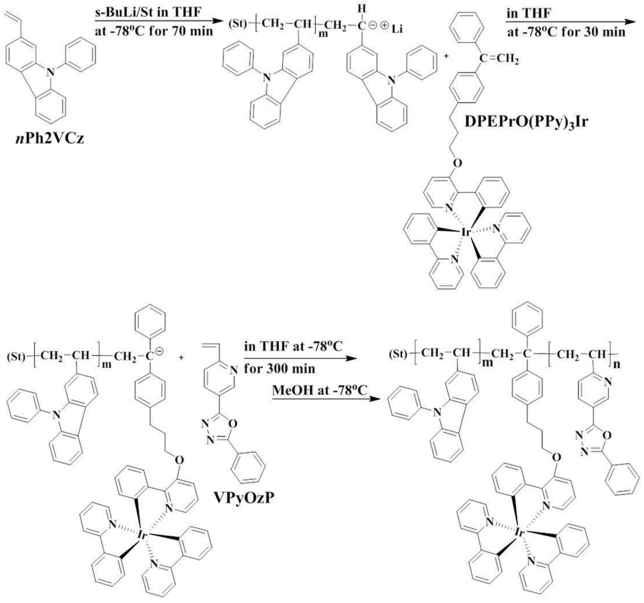

As shown in Scheme 1, to synthesize controlled ambipolar block copolymers, we first synthesized a new carbazole derivative of *n*Ph2VCz by modifying the structure of NVK via the insertion of a phenyl group onto the nitrogen and the incorporation of a vinyl group onto the 2-position of the carbazole unit to overcome the limitations of the anionic polymerization of NVK[14] (see Scheme S1 in the Supporting Information). The anionic polymerization of *n*Ph2VCz was carried out successfully using *n*-BuLi, *s*-BuLi, and *s*-BuLi/styrene ($[s\text{-BuLi}]_0/[St]_0$ = 0.33). The *s*-BuLi/styrene was optimum for the living anionic polymerization of *n*Ph2VCz and resulted in a more controlled molecular weight (M_n) and a narrower molecular weight distribution (M_w/M_n) (20100 and 1.05, respectively) than those obtained with *n*-BuLi (9500 and 1.19) and *s*-BuLi (8700 and 1.11) (see Table S1 in the Supporting Information).

In addition, we designed a DPE derivative with an alkyl chain as a spacer to improve the steric hindrance and solubility at −78 °C for the living anionic polymerization and with an Ir complex at the end of the alkyl chain. DPEPrO(PPy)$_3$Ir, as shown in Scheme 1, was synthesized successfully (see Scheme S3 in the Supporting Information). Next, the DPEPrO(PPy)$_3$Ir was monoadded to each end of the P*n*Ph2VCz chains without any observable side reactions, as shown in Table 1. To the best of our knowledge, this was the first instance in which an Ir-complex unit in DPEPrO(PPy)$_3$Ir was unreactive to attack from the carbanion of the living P*n*Ph2VCz during anionic polymerization. In addition, the location and the concentration of the Ir complex in the block copolymers were completely controlled.

As shown in Scheme 1, a new oxadiazole-containing monomer of VPyOzP was synthesized by introducing a pyridine moiety between the vinyl and the oxadiazole units (see Scheme S4 in the Supporting Information). The addition of the oxadiazole units as a withdrawing group resulted in a decrease in the π-electron densities on the vinyl bonds.[2c] The anionic polymerization of VPyOzP was performed using different initiation systems (*s*-BuLi, *s*-BuLi/DPE, and *s*-BuLi/*n*Ph2VCz/DPE) based on the anionic polymerization of 2VP using *s*-BuLi/DPE under previously reported conditions.[15] Among the initiation systems based on *s*-BuLi, only the anionic polymerization of VPyOzP using *s*-BuLi/*n*Ph2VCz/DPE was successfully optimized, resulting in a controlled M_n and a

Table 1. Synthesis of P*n*Ph2VCz/DPEPrO(PPy)$_3$Ir-*b*-PVPyOzP by Sequential Living Anionic Polymerization in THF at −78 °C

						Block copolymer (homopolymer)					
run	*s*-BuLi/St (mmol)	*n*Ph2VCz (mmol)	DPEPrO (PPy)$_3$Ir (mmol)	VPyOzP (mmol)	time (min)	calcd[a]	$M_n \times 10^{-3}$ obsd[b]	^{1}H NMR[c]	M_w/M_n[b]	yield (%)	(C)$_m$/(I)$_1$/(O)$_n$[d]
PCI	0.045/0.16	1.80	0.059		150	11.5 (10.8)	12.0 (10.6)	12.0	1.07 (1.09)	100	41.3:1:0
PCIO1	0.037/0.14	1.75	0.070	0.33	450	15.8 (13.6)	14.2 (13.5)	14.5	1.13 (1.09)	99	48.1:1:2.69
PCIO2	0.045/0.18	1.48	0.077	0.84	450	15.3 (9.8)	15.9 (10.5)	16.8	1.13 (1.08)	99	37.3:1:23.6
PCIO3	0.048/0.17	0.79	0.068	1.57	450	17.5 (4.4)	18.1 (3.8)	18.6	1.15 (1.07)	98	13.3:1:56.8

[a] M_n (calcd) = MW of 9-phenyl-2-vinyl-9*H*-carbazole (*n*Ph2VCz, C) × [*n*Ph2VCz]/[*s*-BuLi] + MW of (2-phenyl-3-(3-(4-(1-phenylvinyl)phenyl)-propoxy)pyridine)(2-phenylpyridine)$_2$Iridium (DPEPrO(PPy)$_3$Ir, I) + MW of 2-phenyl-5-(6-vinylpyridin-3-yl)-1,3,4-oxadiazole (VPyOzP, O) × [VPyOzP, O]/[*s*-BuLi]. [b] M_n (obsd) and M_w/M_n values were measured by SEC calibration using a polystyrene standard in THF containing 2% triethylamine (TEA, $(C_2H_5)_3N$) as the eluent at 40 °C. [c] Estimated by the ^{1}H NMR signal intensity ratio of the carbazole and oxadiazole protons of P*n*Ph2VCz and PVPyOzP to the methyl protons of the *s*-Bu group. [d] The number of repeating units of each block was determined by ^{1}H NMR.

dx.doi.org/10.1021/mz300121w | *ACS Macro Lett.* 2012, 1, 840−844

narrow M_w/M_n (7700 and 1.11, respectively; see Table S2 in the Supporting Information). These results verified that oxadiazole-containing vinylpyridine derivatives have a living nature if the reactivity of the carbanion can be controlled using *s*-BuLi/*n*Ph2VCz/DPE. Furthermore, we describe, for the first time, the living nature of the oxadiazole-containing monomer.

Based on the following three living conditions, (i) the anionic polymerization of *n*Ph2VCz using *s*-BuLi/styrene, (ii) the Ir-complex unit in DPEPrO$(PPy)_3$Ir unreactive to the attack of the living P*n*Ph2VCz, and (iii) the anionic polymerization of VPyOzP using *s*-BuLi/styrene/*n*Ph2VCz/DPE, as described above, a series of well-defined ambipolar block copolymers (PCIO1−3) were successfully synthesized by the sequential living anionic polymerization shown in Table 1.

The resulting block copolymers have different numbers of repeating units of *n*Ph2VCz (C)/DPEPrO$(PPy)_3$Ir (I)/VpyOzP (O) (C/I/O), such as PCIO1 with C/I/O = 48.1:1:2.69, PCIO2 with 37.3:1:23.6, and PCIO3 with 13.3:1:56.8. The observed M_n of each block copolymer by SEC and ^{1}H NMR was in good agreement with the calculated M_n and the M_w/M_n values of PCIO1, PCIO2, and PCIO3 were narrow, as shown in Table 1. Depending on the different block ratios of carbazole/Ir and oxadiazole, the SEC profiles shifted from poly(*n*Ph2VCz/DPEPrO$(PPy)_3$Ir) (PCI) to PCIO, as shown in Figure 1. This observation confirmed the successful synthesis of the block copolymers by sequential living anionic polymerization.

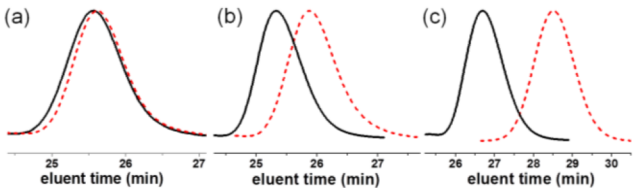

Figure 1. SEC profiles of (a) PCI and PCIO1, (b) PCI and PCIO2, (c) PCI and PCIO3. PCI (poly(*n*Ph2VCz/DPEPrO $(PPy)_3$Ir), dotted line) and PCIO (poly(*n*Ph2VCz/DPEPrO $(PPy)_3$Ir-b-VPyOzP), solid line).

The three block copolymers of PCIO1, PCIO2, and PCIO3 exhibited different ^{1}H and ^{13}C NMR spectra, depending on the block ratios and on the concentrations of P*n*Ph2VCz and poly(2-phenyl-5-(6-vinylpyridin-3-yl)-1,3,4-oxadiazole) (PVPyOzP) in the block copolymers, as shown in Figure 2a,b. The various intensities of the identifying carbazole and oxadiazole spectra were used to estimate the block compositions. Specifically, as the number of oxadiazole units increases in the block copolymers, the intensities of the peaks at 8.94 ppm in the ^{1}H NMR and at 164.6 ppm in the ^{13}C NMR of the oxadiazole spectra were increased. In addition, the intensities of the peaks at 6.1 ppm in the ^{1}H NMR and 109.3 ppm in the ^{13}C NMR spectra of carbazole were reduced. These results further confirmed the synthesis of the three different block copolymers.

The thermal behaviors of P*n*Ph2VCz, PVPyOzP, and PCIO were measured by thermogravimetric analysis (TGA), as shown in Figure 2c, and by differential scanning calorimetry (DSC), as shown in Figure 2d. All of the polymers exhibited excellent thermal stability with an onset (5% weight loss) of decomposition. The decomposition temperature (T_d) of the polymer samples decreased in the following order: P*n*Ph2VCz (T_d = 384 °C) > PCIO1 (377 °C) > PCIO2 (359 °C) > PCIO3 (355 °C) > PVPyOzP (332 °C) as the PVPyOzP-block

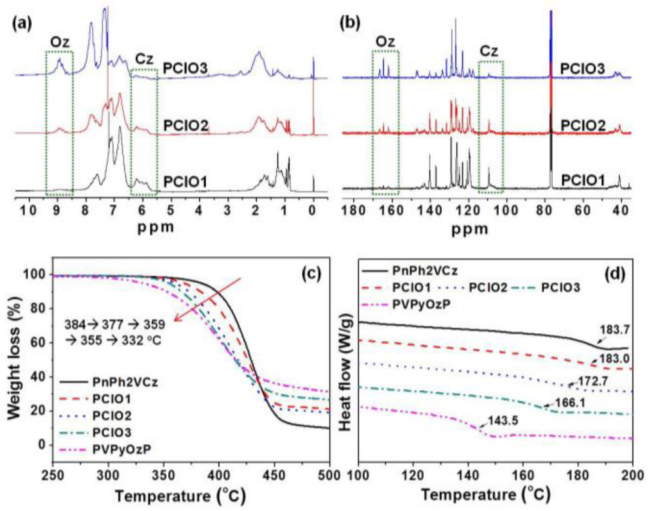

Figure 2. (a) ^{1}H and (b) ^{13}C NMR spectra of P*n*Ph2VCz/DPEPrO$(PPy)_3$Ir-*b*-PVPyOzP with different numbers of repeating units of 48.1:1:2.69 (PCIO1), 37.3:1:23.6 (PCIO2), and 13.3:1:56.8 (PCIO3). (c) The decomposition temperature (T_d) and (d) glass transition temperature (T_g) of P*n*Ph2VCz, PVPyOzP, PCIO1, PClO2, and PCIO3 for different block ratios.

moiety increased in the polymer chain (Figure 2c). The glass transition temperatures (T_g) of P*n*Ph2VCz, PVPyOzP, and PCIO are shown in Figure 2d. The T_gs of P*n*Ph2VCz and PVPyOzP were 183.7 and 143.5 °C, respectively. Each block copolymer of PCIO1, PCIO2, and PCIO3 produced only one T_g. The T_g of PCIO1 (183.0 °C) is similar to that of P*n*Ph2VCz (183.7 °C) because the 18.6 mol % of oxadiazole units in the PCIO1 had only a minimal effect on the T_g of the block copolymer. In contrast, as the oxadiazole units increased in the block copolymer, the T_gs of PCIO2 (172.7 °C) and PCIO3 (166.1 °C) were gradually reduced. High T_d and T_g values are required of polymers for organic electronic devices with high thermal stability. Accordingly, PCIO1, PCIO2, and PCIO3, which have excellent thermal stability, could improve device stability.

Figure 3a shows the normalized UV−vis absorption spectra of PCI, PCIO1, PCIO2, and PCIO3 films. The absorption spectra of these block copolymers exhibited similar bands in the ultraviolet (UV) and visible (vis) regions from 270 to 550 nm because the carbazole, the oxadiazole, the intraligand of the Ir complex ($\pi-\pi^*$), and the metal−ligand charge transfer (^{1}MLCT) transitions of the homoleptic Ir complex were dominated. The maximum absorption wavelength (λ_{max}) of 294 nm for PCIO3 and 302 nm for PCI, PCIO2, and PCIO3 could be assigned to the spin-allowed $\pi-\pi^*$ transition. The weak absorption wavelength of 370−380 nm was assigned to the ^{1}MLCT transition. The ^{1}MLCT transitions of the Ir complexes in these block copolymers are located at the same positions on the Ir$(PPy)_3$-doped PVK and the random copolymer of PVK containing the Ir complex as a side chain.[16] The intensities of the peaks at 278 and 344 nm were altered depending on the block ratio of the block copolymer (Figure 3a). In addition, the UV−vis spectra of PCI, PCIO1, PCIO2, and PCIO3 in chloroform were measured, but no differences could be detected between the wavelengths of the UV−vis spectra of the films and those in chloroform. (see Figure S20 in the Supporting Information).

dx.doi.org/10.1021/mz300121w | *ACS Macro Lett.* 2012, 1, 840−844

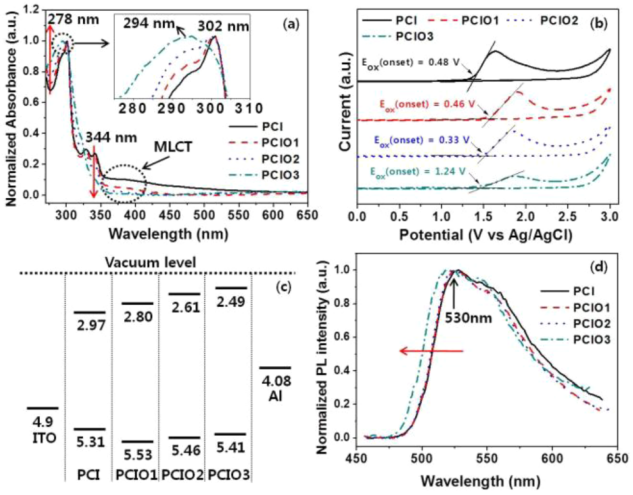

Figure 3. (a) UV−visible absorption spectra, (b) cyclic voltammograms, (c) energy band diagram, and (d) photoluminescence spectra of P*n*Ph2VCz/DPE PrO(PPy)$_3$Ir-*b*-PVPyOzP with the given number of repeating units of 41.3:1:0 (PCI), 48.1:1:2.69 (PCIO1), 37.3:1:23.6 (PCIO2), and 13.3:1:56.8 (PCIO3).

The highest occupied molecular orbitals (HOMO) and lowest unoccupied molecular orbitals (LUMO) level of PCI, PCIO1, PCIO2, and PCIO3 as measured by cyclic voltammetry (CV) are shown in Figure 3b, and the energy band diagram is given in Figure 3c. The CV results verified that the oxidation of the block copolymers began at the carbazole block of a hole-transporting segment. The HOMO energy levels can be calculated based on the ferrocene value of 4.8 eV with respect to the vacuum level.[17] Furthermore, to estimate the LUMO energy levels, the optical energy gap (E_{opt}) was obtained from the absorption onset of the block copolymers. This result demonstrated that the HOMO and LUMO energy levels were predominated by various block ratios in block copolymers (see Table S3 in the Supporting Information).

Figure 3d shows the photoluminescence (PL) spectra of the PCI, PCIO1, PCIO2, and PCIO3 films. The PCI, PCIO1, and PCIO2 exhibited maximum emission at 530 nm, but the block copolymers of PCIO3 showed an emission maximum at 525 nm. The PL spectra of PCI, PCIO1, PCIO2, and PCIO3 in chloroform were also measured to compare with those in film. When the block copolymers of PCI, PCIO1, PCIO2, and PCIO3 in chloroform were excited by 360 nm wavelength, they exhibited a single peak exciplex emission and the same emission maximum at 530 nm, which were different from the bimodal spectra in the film at 530 and 525 nm (see Figure S21 in the Supporting Information). This result indicated that the energy transfer mechanism could be changed by varying the chemical composition of the P*n*Ph2VCz, DPEPrO(PPy)$_3$Ir, and PVPyOzP blocks in the block copolymers as the PVPyOzP block increased. In addition, this varying block composition presumably altered the maximum emission in the film from 530 to 525 nm. The details regarding the blue shift in Figure 3d are not currently clear but will be investigated in the future.

To study the efficiency of the energy transfer, the PLs of P*n*Ph2VCz at the excitation wavelength of 300 nm, DPE PrO(PPy)$_3$Ir at 360 nm, and PVPyOzP at 295 nm were measured (see Figure S22 in the Supporting Information). The maximum emissions of P*n*Ph2VCz, DPEPrO(PPy)$_3$Ir, and PVPyOzP were 366, 530, and 410 nm, respectively. We found that the maximum emission of P*n*Ph2VCz and PVPyOzP was not observed in the PL spectra of each block copolymer, but the dopant emission of DPEPrO(PPy)$_3$Ir was as shown in Figure 3d. This indicates that the emission of P*n*Ph2VCz and PVPyOzP was completely quenched with adequate DPEPrO-(PPy)$_3$Ir, confirming that an efficient Förster energy transfer occurred from P*n*Ph2VCz and PVPyOzP to DPEPrO(PPy)$_3$Ir.

To study the phase separation behavior, the quaternized block copolymers of PCIO1, PCIO2, and PCIO3, which were prepared with HCl in THF, were dissolved in chlorobenzene (1.0 mg/mL, 1.0 wt %). These solutions were then drop-cast onto carbon-coated copper grids and annealed at 240 °C for 50 h. The annealed samples were stained with phosphotungstic acid. Clear microphase separations of the quaternized block copolymers were observed using an energy-filtering transmission electron microscope (EF-TEM), as shown in Figure 4a,

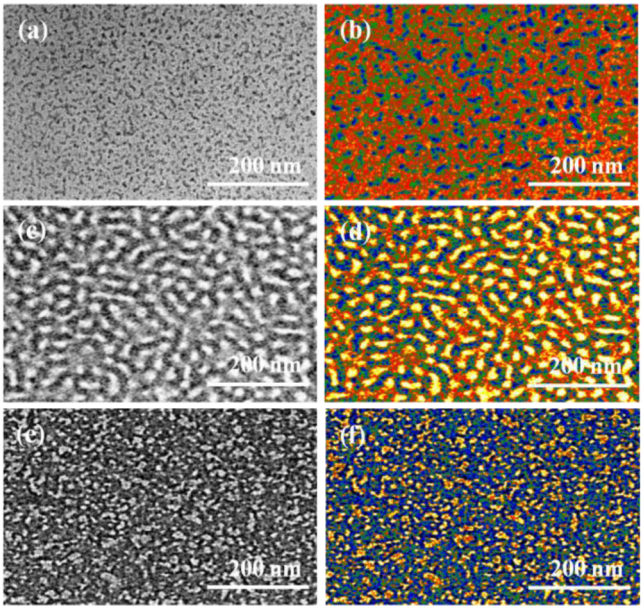

Figure 4. TEM images of P*n*Ph2VCz/DPEPrO(PPy)$_3$Ir-*b*-PVPyOzP block copolymers. (a) PCIO1, (c) PCIO2, and (e) PCIO3. The dark regions stained with phosphotungstic acid are PVPyOzP. IFFT images of (b) PCIO1, (d) PCIO2, and (f) PCIO3 for color after making in temperature.

c, and e. Because quaternization introduced a charge to the PVPyOzP segment, the coil of the PVPyOzP chain was extended as result of Columbic repulsion.[18] In contrast, the block copolymers of PCIO1, PCIO2, and PCIO3 without quaternization with HCl exhibited unclear microphase separations (see Figure S23 in the Supporting Information).

Pixel analysis of the TEM macrographs was performed using Digital Micrograph 3.4 image analysis software (Gatan, Inc. 5933 Coronado Lane, Pleasanton, CA 94588) with a special algorithm for quickly calculating the Fourier transform (FFT) of a source image. After an inverse Fourier transform (IFFT) was performed via calculation of FFT, the images were then recorded in temperature mode (with different colors applied to the images), which is based on the real-space pixels of the analysis area.[19]

Figure 4b, d, and f shows the IFFT images of PCIO1, PCIO2, and PCIO3 for color after making in temperature as reported previously by G. C. Bazan and A. J. Heeger group.[20] In the comparison with the micrographs (Figure 4a, c, and e), as the PVPyOzP composition increases, the dark area in the real

dx.doi.org/10.1021/mz300121w | *ACS Macro Lett.* 2012, 1, 840−844

images increases and the blue regions in the processed images increase. However, the yellowish orange regions decreased, indicating that the blue color represents PVPyOzP, and the yellowish orange color is P*n*Ph2VCz. However, the green areas remain constant in the three images with quantities between those of the blue and yellowish orange regions, indicating that the green color identifies DPEPrO$(PPy)_3$Ir.

In summary, we reported an outstanding strategy to synthesize well-defined block copolymers of P*n*Ph2VCz/DPEPrO$(PPy)_3$Ir-*b*-PVPyOzP by establishing the optimal conditions to fine-tune the nucleophilicity strength of each living polymer in the following order: living P*n*Ph2VCz > DPEPrO$(PPy)_3$Ir > living PVPyOzP, using the monoaddition reactivity of DPEPrO$(PPy)_3$Ir between the P*n*Ph2VCz and PVPyOzP block by sequential living polymerization. In future studies, the ability of these ambipolar block copolymers to control the morphologies and performance of organic electronics will be studied.

■ ASSOCIATED CONTENT

Supporting Information

The details of the synthesis, living anionic polymerization, and block copolymerization of *n*Ph2VCz, DPEPrO$(PPy)_3$Ir, and VPyOzP. Other characterizations including ^{1}H NMR and ^{13}C NMR, DSC, TGA, GC/Mass, and EA. This material is available free of charge via the Internet at http://pubs.acs.org.

■ AUTHOR INFORMATION

Corresponding Author

*E-mail: jslee@gist.ac.kr.

Notes

The authors declare no competing financial interest.

■ ACKNOWLEDGMENTS

This work was supported by the Program for Integrated Molecular Systems (PIMS) and the World Class University (WCU) project at GIST, Korea (Project No. R31-2008-000-100260).

■ REFERENCES

(1) Hadjichristidis, N.; Iatrou, H.; Pitsikalis, M.; Mays, J. *Prog. Polym. Sci.* **2006**, *31*, 1068.

(2) (a) Hirao, A.; Loykulnant, S.; Ishizone, T. *Prog. Polym. Sci.* **2002**, *27*, 1399. (b) Ishizone, T.; Hirao, A.; Nakahama, S. *Macromolecules* **1993**, *26*, 6964. (c) Kang, N.-G.; Changez, M.; Lee, J.-S. *Macromolecules* **2007**, *40*, 8553. (d) Kang, B.-G.; Kang, N.-G.; Lee, J.-S. *Macromolecules* **2010**, *43*, 8400. (e) Kang, B.-G.; Kang, N.-G.; Lee, J.-S. *J. Polym. Sci., Part A: Polym. Chem.* **2011**, *49*, 5199.

(3) (a) Mulvaney, J. A.; Londrigan, M. *J. Polym. Sci., A* **1972**, *10*, 2487. (b) Natori, I. *Macromolecules* **2006**, *39*, 6017.

(4) (a) Cho, Y.-S.; Kim, S.-W.; Ihn, C.-S.; Lee, J.-S. *Polymer* **2001**, *42*, 7611. (b) Cho, Y.-S.; Lee, J.-S.; Cho, G. *Polymer* **2002**, *43*, 1197. (c) Cho, Y.-S.; Lee, J.-S. *Macromol. Rapid Commun.* **2001**, *22*, 638.

(5) Rembaum, A.; Hermann, A. M.; Haack, R. *Polym. Sci. B* **1967**, *5*, 407.

(6) (a) Tao, Y.; Wang, Q.; Yang, C.; Wang, Q.; Zhang, Z.; Zou, T.; Qin, J.; Ma, D. *Angew. Chem., Int. Ed.* **2008**, *47*, 8104. (b) Ponomarev, O. A.; Surov, Y. N.; Pivnenko, N. S.; Popova, N. A.; Fedyunyaeva, I. A. *Chem. Heterocycl. Compd.* **1997**, *33*, 707. (c) Kido, J.; Shionoya, H.; Nagai, K. *Appl. Phys. Lett.* **1995**, *67*, 2281.

(7) (a) Li, X.-C.; Cacialli, F.; Giles, M.; Crüner, J.; Friend, R. H.; Holmes, A. B.; Moratti, S. C.; Yong, T. M. *Adv. Mater.* **1995**, *7*, 898. (b) Cacialli, F.; Li, X.-C.; Friend, R. H.; Moratti, S. C.; Holmes, A. B. *Synth. Met.* **1995**, *75*, 161. (c) Greczmiel, M.; Strohriegl, P.; Meier, M.; Brütting, W. *Macromolecules* **1997**, *30*, 6042.

(8) (a) Ishizone, T.; Utaka, T.; Ishino, Y.; Hirao, A.; Nakahama, S. *Macromolecules* **1997**, *30*, 6458. (b) Hirao, A.; Higashihara, T.; Nagura, M.; Sakurai, T. *Macromolecules* **2006**, *39*, 6081.

(9) (a) Thompson, B.; Fréchet, J. M. J. *Angew. Chem., Int. Ed.* **2008**, *47*, 58. (b) Kang, N.-G.; Cho, B.; Kang, B.-G.; Song, S.; Lee, T.; Lee, J.-S. *Adv. Mater.* **2012**, *24*, 385. (c) Hahm, S. G.; Kang, N.-G.; Kwon, W.; Kim, K.; Ko, Y.-K.; Ahn, S.; Kang, B.-G.; Chang, T.; Lee, J.-S.; Ree, M. *Adv. Mater.* **2012**, *24*, 1062. (d) Lindner, S. M.; Hüttner, S.; Chiche, A.; Thelakkat, M.; Krausch, G. *Angew. Chem., Int. Ed.* **2006**, *45*, 3364. (e) Sommer, M.; Lang, A. S.; Thelakkat, M. *Angew. Chem., Int. Ed.* **2008**, *47*, 7901. (f) Sommer, M.; Lindner, S. M.; Thelakkat, M. *Adv. Funct. Mater.* **2007**, *17*, 1493. (g) Fang, Y.-K.; Liu, C.-L.; Chen, W.-C. *J. Mater. Chem.* **2011**, *21*, 4778.

(10) (a) Ma, B.; Kim, B. J.; Deng, L.; Poulsen, D. A.; Thompson, M. E.; Fréchet, J. M. J. *Macromolecules* **2007**, *40*, 8156. (b) Deng, L.; Furuta, P. T.; Garon, S.; Li, J.; Kavulak, D.; Thompson, M. E.; Fréchet, J. M. J. *Chem. Mater.* **2006**, *18*, 386. (c) Poulsen, D. A.; Kim, B.; Ma, B.; Sebastian, C. S.; Fréchet, J. M. J. *Adv. Mater.* **2010**, *22*, 77. (d) Furuta, P. T.; Deng, L.; Garon, S.; Thompson, M. E.; Fréchet, J. M. J. *J. Am. Chem. Soc.* **2004**, *126*, 15388. (e) Wang, X. Y.; Prabhu, R. N.; Schmehl, R. H.; Weck, M. *Macromolecules* **2006**, *39*, 3140.

(11) Deng, L.; Furuta, P. T.; Garon, S.; Li, J.; Kavulak, D.; Thompson, M. E.; Fréchet, J. M. J. *Chem. Mater.* **2006**, *18*, 386.

(12) (a) Bates, F. S.; Fredrickson, G. H. *Annu. Rev. Phys. Chem.* **1990**, *41*, 525. (b) Bates, F. S.; Fredrickson, G. H. *Phys. Today* **1999**, *52*, 32.

(13) (a) Bates, F. S. *Science* **1991**, *251*, 898. (b) Nguyen, T. Q.; Kwong, R. C.; Thompson, M. E.; Schwartz, B. *J. Appl. Phys. Lett.* **2000**, *76*, 2454. (c) Alam, M. M.; Tonzola, C. J.; Jenekhe, S. A. *Macromolecules* **2003**, *36*, 6577. (e) Kim, J. S.; Ho, P. K. H.; Murphy, C. E.; Friend, R. H. *Macromolecules* **2004**, *37*, 2861. (f) Xia, Y. J.; Friend, R. H. *Adv. Mater.* **2006**, *18*, 1371.

(14) Limburg, W. W.; Yanus, J. F.; Williams, D. J.; Goedde, A. O.; Pearson, J. M. *J. Polym. Sci.: Polym. Chem. Ed.* **1975**, *13*, 1133.

(15) (a) Liu, F.; Eisenberg, A. *Angew. Chem., Int. Ed.* **2003**, *42*, 1404. (b) Quirk, R. P.; Galvan-Corona, S. *Macromolecules* **2001**, *34*, 1192. (c) Watanabe, H.; Amemiya, T.; Shimura, T.; Kotaka, T. *Macromolecules* **1994**, *27*, 2336. (d) Shin, Y.-D.; Han, S.-H.; Samal, S.; Lee, J.-S. *J. Polym. Sci., Part A: Polym. Chem.* **2005**, *43*, 607.

(16) (a) Lee, C.-L.; Lee., K. B.; Kim, J.-J. *Appl. Phys. Lett.* **2000**, *77*, 2280. (b) Lee, C.-L.; Kang, N.-G.; Cho, Y.-S.; Lee, J.-S.; Kim, J.-J. *Opt. Mater.* **2002**, *21*, 119.

(17) Hwang, S.-W.; Chen, Y. *Marcromolecules* **2002**, *35*, 5438.

(18) (a) Chumg, B.; Choi, M.; Ree, M.; Jung, J. C.; Zin, W. C.; Chang, T. *Macromolecules* **2006**, *39*, 684. (b) Roiter, Y.; Minko, S. *J. Am. Chem. Soc.* **2005**, *127*, 15688.

(19) (a) Fan, G. Y.; Cowley, J. M. *Ultramicroscopy* **1985**, *17*, 345. (b) Zhang, X.; Hudson, S. D.; DeLongchamp, D. M.; Gundlach, D. J.; Heeney, M.; McCulloch, I. *Adv. Funct. Mater.* **2010**, *20*, 4098. (c) Reimer, L.; Kohl, H. In *Transmission electron microscopy : physics of image formation and microanalysis*, 3rd ed.; Springer Verlag, Berlin; New York, 1993; Chap. Xiii, p545.

(20) Sun, Y.; Welch, G. C.; Leong, W. L.; Takacs, C. J.; Bazan, G. C.; Heeger, A. J. *Nat. Mater.* **2011**, *11*, 44.